*Title Page

Long-term photosynthetic CO_2 removal from biogas and flue-gas: exploring the potential of closed photobioreactors for high-value biomass production

Alma Toledo-Cervantes[1,2], Tamara Morales[1], Álvaro González[1], Raúl Muñoz[1], Raquel Lebrero[1]*

1.-Department of Chemical Engineering and Environmental Technology, Valladolid, Dr. Mergelina s/n., Valladolid 47011, Spain.

2.- Department of Chemical Engineering, CUCEI-Universidad de Guadalajara, Blvd. M. García Barragán 1451, C.P. 44430, Guadalajara, Jalisco, México.

*Corresponding author: raquel.lebrero@iq.uva.es

*Graphical Abstract

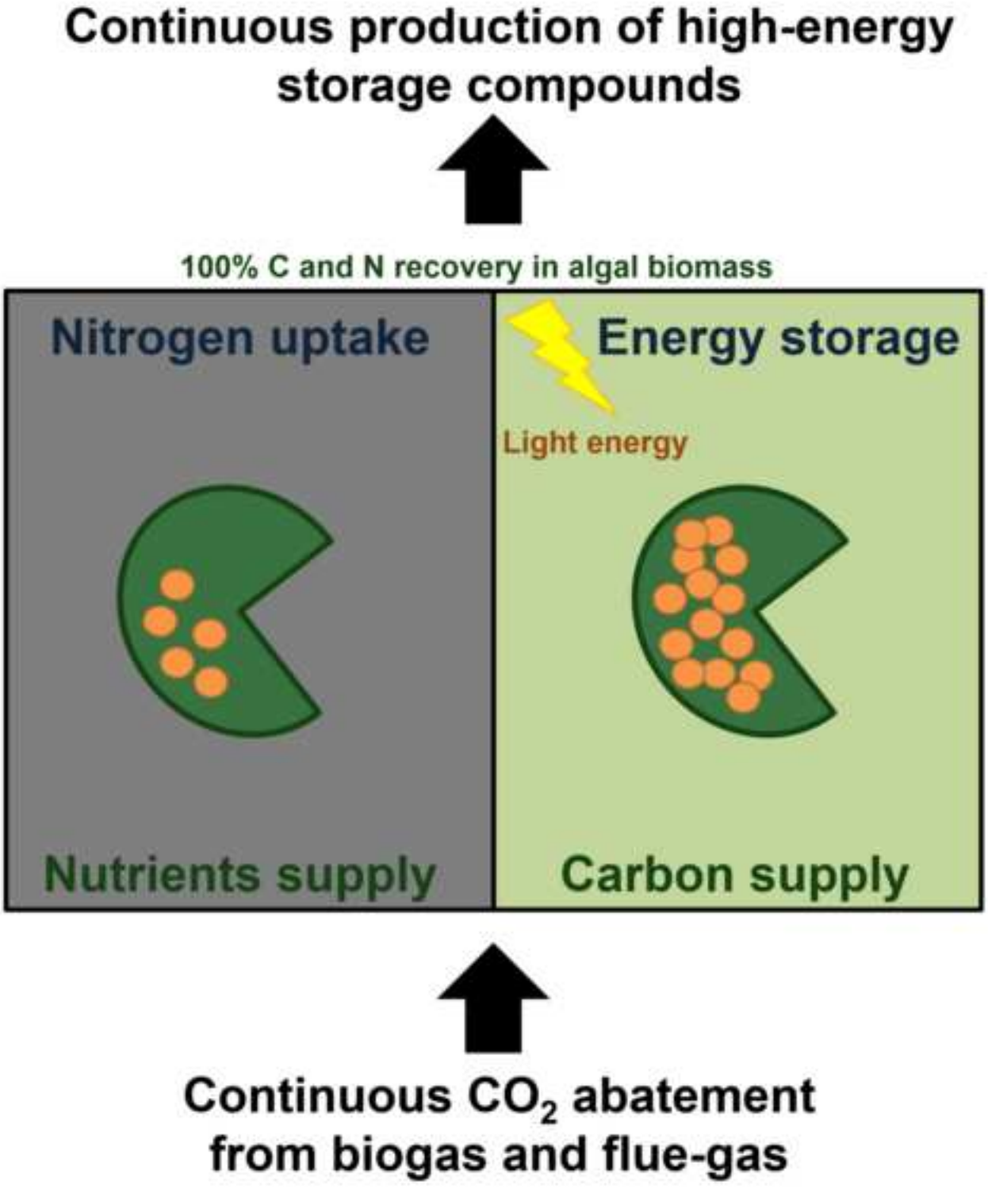

Highlights

- CO_2 abatement from biogas and flue-gas was studied in a tubular photobioreactor
- A feast-famine regime was applied for continuous production of high-energy storage compounds
- CO_2 removals > 98% and complete C and N recovery as biomass was achieved
- Microalgae consumed nitrogen in the dark period regardless of the N source
- The N-dark feeding strategy increased the carbohydrates productivity by 1.7 times

Long-term photosynthetic CO_2 removal from biogas and flue-gas: exploring the potential of closed photobioreactors for high-value biomass production

Alma Toledo-Cervantes[1,2], Tamara Morales[1], Álvaro González[1], Raúl Muñoz[1], Raquel Lebrero[1]*

1.-Department of Chemical Engineering and Environmental Technology, Valladolid, Dr. Mergelina s/n., Valladolid 47011, Spain.

2.- Department of Chemical Engineering, CUCEI-Universidad de Guadalajara, Blvd. M. García Barragán 1451, C.P. 44430, Guadalajara, Jalisco, México.

*Corresponding author: raquel.lebrero@iq.uva.es

Abstract

The long-term performance of a tubular photobioreactor interconnected to a gas absorption column for the abatement of CO_2 from biogas and flue-gas was investigated. Additionally, a novel nitrogen feast-famine regime was implemented during the flue-gas feeding stage in order to promote the continuous storage of highly-energetic compounds. Results showed effective CO_2 (~98%) and H_2S (~99%) removals from synthetic biogas, supported by the high photosynthetic activity of microalgae which resulted in an alkaline pH (~10). In addition, CO_2 removals of 99 and 91% were observed during the flue-gas operation depending on the nutrients source: mineral salt medium and digestate, respectively. A biomass productivity of ~8 g m^{-2} d^{-1} was obtained during both stages, with a complete nitrogen and carbon recovery from the cultivation broth. Moreover, the strategy of feeding nutrients during the dark period promoted the continuous accumulation of carbohydrates, their concentration increasing from 22% under normal nutrition up to 37% during the feast-famine cycle. This represents a productivity of ~3 $g_{carbohydrates}$ m^{-2} d^{-1}, which can be further valorized to contribute to the economic sustainability of the photosynthetic CO_2 removal process.

Keywords: Algal-bacterial technology; Biogas upgrading; Carbohydrates production; CO_2 abatement; Photobioreactors.

1. Introduction

Carbon dioxide (CO_2) represents nowadays the most important greenhouse gas (GHG), with ~77% of the total GHG emissions worldwide and an annual atmospheric concentration increase of 0.5% over the last decade (López *et al*., 2014). In addition, the amount of CO_2 emitted from anthropogenic sources has increased from 22 Gt in 1990 to 33 Gt in 2010, and it is expected to reach 41 Gt by 2030 (World Bank, 2014; United Nations, 2015). From these anthropogenic CO_2 emissions, ~93.5% are produced from the combustion of fossil fuels, with a typical concentration in the emitted gases ranging from 5 to 20% (Raeesossadati *et al*., 2014; Warmuzinski *et al*., 2014). Energy production from biogas also constitutes an important source of anthropogenic CO_2 emissions (CO_2 content in raw biogas can vary from 15 up to 60%), which production in Europe is expected to reach 18-20 million m^3 by 2030 (Muñoz *et al*., 2015). The detrimental effects of this GHG on the environment (*i.e.* global warming, modification of the pH of oceans, etc.) demand the implementation of cost-effective technologies for CO_2 removal from industrial emissions. In the particular case of biogas, the abatement of the CO_2 not only entails environmental benefits but also contributes to the upgrading of this biofuel, decreasing its transportation costs and increasing the energy content.

Conventional physical/chemical technologies for CO_2 removal from flue-gas or biogas, such as scrubbing, adsorption, or cryogenic separation, have been widely implemented due to the extensive knowledge on their design and operation and the high removal efficiencies achieved. However, only biological technologies offer a low environmental impact, besides reducing the operating costs associated to the treatment process. In this regard, CO_2-capturing biotechnologies supported by the photosynthetic activity of microalgae in photobioreactors allow for the removal of CO_2 in a cost-effective, environmentally friendly way (Raeesossadati *et al*., 2014; Muñoz *et al*. 2015). In this

60 microalgae-based process, the CO_2 is transferred from the gas to the liquid phase when
61 the flue-gas/biogas is sparged into the cultivation broth, being subsequently fixed by
62 microalgae during photosynthesis in the presence of light. Therefore, the CO_2 is not
63 only removed from the gas preventing its emission to the atmosphere, but the C-CO_2 is
64 recovered as valuable algal biomass, which can be further valorized (Raeesossadati *et*
65 *al*., 2014; Muñoz *et al*. 2015). Moreover, the necessary nutrients for microalgae growth
66 can be supplemented from wastewaters, which increases the environmental
67 sustainability of the process (Park and Cragss, 2010). However, most wastewaters are
68 characterized by a low C/N/P ratio compared to that needed for microalgae growth
69 (20:8:1 for urban wastewaters *vs* 106:16:1 to ensure balanced algae growth), therefore
70 carbon limitation usually hinders nutrient recovery from wastewater. In this sense, CO_2
71 supply into the cultivation broth from biogas or flue-gas increases the availability of
72 inorganic carbon, enhancing biomass productivity, ensuring complete nutrient recovery
73 from wastewater and mitigating microalgae pH-derived inhibition (Arbid *et al*., 2013;
74 Posadas *et al*., 2015).
75 The potential of algal-bacterial symbiosis for biogas (Toledo-Cervantes *et al*., 2016;
76 Toledo-Cervantes *et al*., 2017b) or flue-gas (Posadas *et al*. 2015) purification combined
77 to wastewater treatment has been already studied and demonstrated in open
78 photobioreactors. However, few studies have focused on the implementation of this
79 process in closed photobioreactors, which offers higher photosynthetic efficiencies by
80 avoiding light limitation, enhanced biomass productivities and better CO_2 mass transfer
81 (Chisti, 2007; Arbid *et al*., 2013). On the other hand, this photosynthetic CO_2-abatement
82 process can be further optimized by implementing nutrient supplementation strategies to
83 promote the production of storage compounds in the algal biomass (Mooij *et al*., 2013).
84 In this context, the production of a biomass with a high content in the metabolites of

interest will increase the economic sustainability of the process (Toledo-Cervantes *et al.*, 2017a).

This work aimed at evaluating the long-term performance of a tubular photobioreactor interconnected to a CO_2 absorption column for the abatement of CO_2 from biogas and flue-gas. Furthermore, a feast-famine regime was implemented in order to exploit the cyclic nitrogen absence for the continuous production of high-energy storage compounds.

2. Materials and methods

2.1 Experimental system

The experimental system consisted of a tubular photobioreactor interconnected to a mixing chamber and a CO_2 absorption column (AC) (Figure 1). The tubular photobioreactor was composed of 12 tubes of 6 cm inner diameter and 94 cm of length, with a total volume of 45.5 L. The mixing chamber (60 cm height, 50 cm width and 35 cm length) had a working volume of 60 L. The absorption column was 2 m height (1.73 m water column) with an internal diameter of 5 cm and a working volume of 3.5 L. Two sets of high intensity LED PCBs were placed at both sides of the photobioreactor to provide a photosynthetic active radiation (PAR) of ~1100 μmol m^{-2} s^{-1}. Light:dark cycles of 12:12 h of the PAR were fixed. The cultivation broth was re-circulated through the tubular photobioreactor and the mixing chamber at a linear velocity of 0.5 m s^{-1}. The absorption column was operated by supplying co-currently the cultivation broth from the mixing chamber and biogas/flue-gas (through a stainless steel diffuser of 2 μm pore size) at the bottom of the column. The operating parameters such as liquid and gas flow rates of the absorption column and nutrients/digestate solution flow rates are described in section 2.2.

2.2 Experimental system operation

2.2.1 Operation with biogas (A):

Prior operation, an abiotic CO_2/H_2S removal test was performed in order to determine the optimum liquid to gas flow rates (L/G) ratio in the AC, which maximizes the CO_2 and H_2S removal from biogas without compromising the CH_4 content and the quality of the upgraded biogas due to N_2 and O_2 desorption (Toledo-Cervantes *et al*., 2016). The biogas used was a synthetic mixture of 29.5% CO_2, 0.5% H_2S and 70% CH_4. The liquid phase was a modified Bristol medium (final pH = 7.5) (g L^{-1}): $NaNO_3$ (1.5), $CaCl_2$ $2H_2O$ (0.025), $MgSO_4 \cdot 7H_2O$ (0.075), K_2HPO_4 (0.075), KH_2PO_4 (0.175), NaCl (0.025), and 1 mL L^{-1} of a micronutrient solution (2.86 g L^{-1} H_3BO_3, 1.81 g L^{-1} $MnCl_2$ $4H_2O$, 0.22 g L^{-1} $ZnSO_4$ $7H_2O$, 0.39 g L^{-1} Na_2MoO_4 $2H_2O$, 0.079 g L^{-1} $CuSO_4$ $5H_2O$ and 49.4 mg L^{-1} $Co(NO_3)_2$ $6H_2O$). The liquid recirculation rates tested were 60, 150, 300 and 450 mL min^{-1} while the biogas flow rate was set at 40 mL min^{-1}. Hence, L/G ratios ranging from 1 to 11 were studied. The AC was allowed to stabilize for two times the hydraulic retention time prior monitoring the upgraded biogas composition by GC-TCD.

The system was inoculated with the microalgae *Acutudesmus obliquus* at an initial suspended solids concentration (SST) of 0.1 g L^{-1}, and operated for biogas upgrading during 150 days. The CO_2 contained in the synthetic biogas previously described was used as carbon source for microalgae growth, while nutrients were supplied by means of the modified Bristol medium. During stage IA (from day 1 to 54) the synthetic biogas was fed during the illuminated period into the absorption column at a flow rate of 40 mL min^{-1} and the liquid broth was recirculated through the AC at a flow rate of 400 mL min^{-1} (L/G ratio = 10). The modified Bristol medium was fed into the mixing chamber

at a flow rate of 3 mL min^{-1} (hydraulic retention time, HRT = 50 d) during the light period. The feed flow rate was selected according to the nitrogen load needed for the complete photosynthetic fixation of the CO_2 contained in the biogas, assuming a biomass composition of 50 % of carbon and 10 % of nitrogen (Groobelar, 2004). From days 54 to 77 (stage IIA) the synthetic biogas was continuously fed into the absorption column (24 h gas feeding), therefore the mineral medium flow rate was increased to 6 mL min^{-1} (HRT= 25 d). During this stage, both the gas and the liquid flow rates through the AC were maintained constant (L/G ratio = 10). Finally, in Stage IIIA (days 77 to 150) the synthetic biogas was only fed during the light period at 80 mL min^{-1} (L/G ratio = 5) while the mineral medium feeding flow rate was kept at 6 mL min^{-1} (HRT= 25 d).

2.2.2 Operation with flue-gas (B):

During experiment B, a synthetic flue-gas composed of 20% of CO_2 and 80% of N_2 was used as carbon source for the growth of microalgae. During Stage IB (from day 151 to 280) the synthetic flue-gas was fed at 50 mL min^{-1} during the light period (L/G = 5). The mineral medium previously described was modified by decreasing the $NaNO_3$ concentration to 0.75 g L^{-1} and the nitrogen load rate was adjusted to the photosynthetic fixation of the CO_2 contained in the flue-gas. Therefore, the nutrient solution was fed into the mixing chamber at a flow rate of 10 mL min^{-1} (HRT= 15 d). From days 284 to 297 (Stage IIB) no nitrogen source was added to the mineral medium in order to decrease the concentration of nitrogen in the cultivation broth to the non-assimilative nitrogen concentration (<2 mg-N L^{-1}). No further modifications were implemented during this period.

During stage IIIB (days 297 to 336) mineral medium was fed at the same HRT (15 d) only during the dark period in order to promote the production of high-energy

compounds. The nitrogen load was set at 511 mg d^{-1} based on the biomass productivity observed in stage IIB and considering a biomass nitrogen content of 7% (experimental data from stage IB). No nutrient was supplemented during the light period in which the flue-gas was fed (Mooij *et al*., 2015). From days 336 to 380 (Stage IVB) the synthetic nutrient solution was substituted by a diluted anaerobic digestate solution obtained from the wastewater treatment plant of Valladolid city (Spain), with an average composition of total nitrogen (TN), inorganic carbon (IC) and total phosphorus (TP) of 660 ± 46, 524 ± 49 and 48 ± 3 mg L^{-1}, respectively. The digestate feeding flow rate was adjusted to ensure the same nitrogen load as in Stage IIIB.

The steady state biomass chemical (C, N, P, and S) and biochemical (proteins, carbohydrates, lipids, and ashes) composition were determined at the end of the light and dark periods two times a week.

During both operating periods (*i.e.* A and B), the biomass concentration, measured as TSS, was determined twice a week. The temperature and dissolved oxygen concentration (DO) in the cultivation broth were daily in-situ monitored. Inlet (biogas and flue-gas) and outlet (upgraded biogas and treated gas) gas samples were drawn twice a week to analyze the composition by GC-TCD. The inlet and outlet gas flow rates in the AC were also periodically measured in order to perform the gas mass balance. Samples of 100 mL of the cultivation broth and mineral medium or diluted digestate were taken twice a week to determine the pH and concentrations of TN, IC, nitrate (NO_3^-), sulfate (SO_4^{2-}) and phosphate (PO_4^{3-}). The population of microalgae in the photobioreactor was identified by microscopic observation at the end of each steady state.

184 **2.3 Analytical methods**

185 Biomass concentration was determined by dry weight (105 ºC, 24 h). NO_3^-, PO_4^{3-} and
186 SO_4^{2-} concentrations were analyzed by HPLC-IC according to Serejo *et al*., (2015).
187 Dissolved IC and TN concentrations were determined using a Shimadzu TOC-VCSH
188 analyzer (Japan) equipped with a TNM-1 chemiluminescence module. The PAR was
189 measured with a LI-190 quantum sensor and recorded with a LI-250A light meter
190 (Lincoln, Nebraska, USA). The pH was monitored with a pH meter Eutech Cyberscan
191 pH 510 (Eutech instruments, The Netherlands), while the DO concentration was
192 measured with an Oxi 330i oximeter (WTW, Germany). The gas composition (CO_2,
193 H_2S, O_2, N_2, and CH_4 concentrations) was analyzed by GC-TCD according to Posadas
194 *et al.* (2015). Microalgae identification was performed by microscopic observations
195 (OLYMPUS IX70, USA) after sample fixation with 5% of lugol acid.

196 The carbohydrate and protein content of the biomass was determined according to the
197 methodology described in Dubois *et al*. (1956) and Lowry *et al*. (1951), respectively.
198 For carbohydrates determination, 1.5 mL of cultivation broth (biomass concentration
199 ~0.2 g L^{-1}) was mixed with 4 mL of H_2SO_4 1 M. Afterwards, the sample was heated for
200 20 min at 100 ºC and centrifuged for 5 min at 10000 rpm. A volume of 0.5 mL of the
201 supernatant was mixed with 0.5 mL of a 5% phenol solution and stood for 40 min. After
202 that period, 2.5 mL of concentrated H_2SO_4 were added, and then the optical density was
203 determined at 485 nm. Protein content was measured by mixing 1 mL of the cultivation
204 broth and 1 mL of NaOH 1 N and heated at 100 ºC for 20 min. After centrifugation (5
205 min at 10000 rpm), 0.4 mL of the supernatant were mixed with 2 mL of a solution
206 composed of 1:25 (v/v) of 5% (w/v) Na_2CO_3 and 0.5% (w/v) $CuSO_4$ in 1% (p/v) sodium
207 potassium tartrate. The mixture was stood for 10 min. Subsequently, 0.4 mL of 1 N
208 Folin & Ciocalteu's phenol reagent was added and kept in dark for 30 min. The optical

density of the preparation was then read at 750 nm. Total lipids were determinate by direct extraction in an automatic Soxhlet extraction unit (SER 148 Series, Velp Scientifica) using hexane as solvent. The extraction conditions were set as follows: extraction temperature 130°C, immersion time 60 min, and solvent recovery time 120 min. The ashes content was determine as volatile solids according to Standard methods (Eaton *et al*., 2005). Finally, the elemental composition of biomass was determined using a CHNS analyzer (LECO CHNS-932) for C and N content, while an Inductively Coupled Plasma-Optical Emission Spectrometer (ICP-OES, Varian 725-ES) was used for P and S content determination.

3. Results and Discussions

3.1. Biogas upgrading

3.1.1. Abiotic removal of CO_2 and H_2S

Table 1 shows the upgraded biogas composition and removal efficiencies obtained at different liquid to biogas flow rate ratios during the preliminary abiotic test. Maximum mass transfer efficiencies for both CO_2 and H_2S were obtained at an L/G of 11 (~91 and 99%, respectively). Similar studies have reported higher CO_2 and H_2S removal efficiencies (REs) of 98.8 ± 0.2 and 97.1 ± 1.4%, respectively, regardless of the L/G ratio tested but using the algal-bacterial broth at a pH of 10 (Toledo-Cervantes, 2016). Furthermore, Serejo *et al*. (2015) obtained a CO_2-RE of 95 ± 2% at L/G ratios above 15 because of the lower pH (≈7.9) of the cultivation broth. During these studies, higher N_2 (7-25%) and O_2 (3-7%) concentrations were observed in the upgraded biogas as a result of the photosynthetic activity (DO ≥ 8 mg-O_2 L^{-1}) and the nitrogen concentration in the liquid broth (~14 mg-N_2 L^{-1}), and its subsequent stripping from the cultivation broth. In this context, closed photobioreactors are considered a viable alternative to open systems

for preventing desorption of nitrogen in the absorption column, since the cultivation broth is not in contact with the atmosphere. However, to the best of our knowledge, this is the first study reporting the upgraded biogas composition in a closed tubular photobioreactor (Table 1). Maximum methane concentrations of ~85% were achieved in the abiotic test since methane content in the upgraded biogas is compromised between the low nitrogen desorption and the low CO_2 removal reached at L/G ratios <11 and a pH of the cultivation broth of 7.5. In this sense, it is worth noticing that, since H_2S and CO_2 are acidic gases, higher absorption of these components from the biogas is expected under biotic conditions as a result of the increase in pH by algal photosynthetic activity.

3.1.2. Photosynthetic CO_2 and H_2S removal from biogas

During stage IA, CO_2 and H_2S were effectively removed from biogas at 97.6 ± 0.4 and 98.3 ± 0.0%, respectively (Figure 2a). As previously discussed, the high removals here observed were supported by the photosynthetic activity of microalgae, which allowed for a dissolved oxygen concentration of 8.1 ± 1.1 mg-O_2 L^{-1} and a pH of 10.7 ± 0.5. Some studies have previously reported efficient biogas upgrading by alkalophilic microalgae cultivation or by using highly alkaline digestate (Franco-Morgado *et al*., 2017; Toledo-Cervantes *et al*., 2016, 2017b). However, during this study, only the high photosynthetic activity of microalgae supported the alkaline pH needed for the effective transfer of CO_2 and H_2S from the gas phase into the cultivation broth. Under these conditions, the upgraded biogas had a composition of CO_2 0.4 ± 0.4 %, H_2S 0.01 ± 0.01%, O_2 8.3 ± 2.9%, N_2 7.7 ± 2.9% and CH_4 83.6 ± 1.8%, which is suitable for electricity production in motor generators (Figure 2b).

During stage IIA, the operating strategy of feeding the biogas continuously decreased the pH of the cultivation broth to 7.2 ± 0.7. This acidic condition and the likely toxic effect of the H_2S inhibited the microalgae activity, which was confirmed by the low DO concentration observed, 3.6 ±1.8 mg-O_2 L^{-1}. Despite some studies have demonstrated that biogas containing up to 0.5% of H_2S (5000 ppm_v) does not inhibit microalgae growth, González-Sánchez and Posten (2017) have recently reported inhibitory effects at concentrations higher than 200 ppm_v. These results were associated to the closed configuration of the photobioreactor, which likely induced the accumulation of HS^- in the cultivation broth during the dark period when dissolved oxygen concentration decreases, thus preventing further HS^- oxidation. However, the H_2S removal remained similar to that observed in stage IA at 99.7 ± 0.0 %, due its higher solubility compared to that of CO_2 (Henry law constants: $H_2S = 1 \times 10^{-3}$ vs. $CO_2 = 3.3 \times 10^{-4}$ mol m^{-3} Pa^{-1}) (Sanders, 1999). This promotes the mass transfer of H_2S to the liquid phase, leading to a toxic effect at low DO concentrations. In contrast, because of the decrease in pH driven by the low photosynthetic activity, the CO_2 removal decreased to 57.0 ± 0.1 % (Figure 2a). It is worth noticing that similar photosynthetic biogas upgrading studies have reported CO_2 removals in the range of 50–98.8% depending on the alkalinity of the cultivation broth and the environmental conditions in high rate algal ponds (both indoors and outdoors) (Franco-Morgado *et al*., 2017; Posadas *et al*., 2017; Toledo-Cervantes *et al*., 2017). These findings highlight the need of pH control in this bioreactor configuration to avoid the deterioration of the CO_2 removal performance.

In order to recover the cultivation broth conditions suitable for biogas upgrading, the biogas inlet flow was doubled during the illuminated period (stage IIIA). This operating strategy allowed increasing the pH up to 10.0 ± 0.2 and the CO_2 and H_2S removals stabilized at 98.3 ± 0.0 and 99.9 ± 0.0%, respectively (Figure 2a). Under these favorable

conditions, the upgraded biogas had a similar composition of that obtained in stage IA: CO_2 1.8 ± 3.4%, H_2S 0.00 ± 0.00, O_2 9.6 ± 3.3%, N_2 6.0 ± 2.2% and CH_4 82.6 ± 3.8% (Figure 2b). The slightly higher oxygen concentration recorded in the upgraded biogas was correlated with the higher DO concentration in the cultivation broth (10.8 ± 1.2 mg-O_2 L^{-1}) when compared to stage IA.

Regarding algal biomass production, the photobioreactor operation at a HRT = 50 d during stage IA lead to a biomass productivity of 2.5 ± 0.2 g m^{-2} d^{-1}, which entailed nitrogen and carbon recoveries of 56.6 ± 3.1% and 50.5 ± 4.5%, respectively. In stage IIA, the lower HRT of 25 days resulted in an increase in biomass concentration from 1.6 ± 0.1 to 2.2 ± 0.1 g L^{-1}, that corresponded to a biomass productivity of 7.2 ± 0.3 g m^{-2} d^{-1}. During this period, the mass balance showed that 86.2 ± 2.6% of the C-CO_2 removed from biogas and 81.4 ± 3.2% of the nitrogen fed were recovered as biomass. Finally, in stage IIIA, the doubling of the carbon load during the illuminated period allowed increasing the biomass concentration to 2.5 ± 0.1 g L^{-1} together with a biomass productivity of 8.0 ± 0.2 g m^{-2} d^{-1}. Under these conditions, a complete nitrogen and carbon recovery as algal biomass was observed. These results confirm the potential of tubular photobioreactors for effective C-CO_2 recovery from biogas and nutrients removal. Furthermore, closed photobioreactors are recognized for the higher biomass productivities achieved in comparison with open systems. However, due to the lack of standardization of the reported values, volumetric productivities (g L^{-1} d^{-1}) are often used for closed photobioreactors instead of areal productivity (g m^{-2} d^{-1}), which hampers a fair comparison between both configurations. In this sense, while productivities of 0.06 g L^{-1} d^{-1} have been reported for closed photobioreactors treating biogas (Meier *et al.*, 2016), productivities in the range of 2.2 – 15 g m^{-2} d^{-1} are commonly achieved in open systems, which in fact represents volumetric productivities between 0.015 and 0.1

308 g L d^{-1} (Toledo-Cervantes *et al*., 2016; Posadas *et al*., 2017; Toledo-Cervantes *et al*.,
309 2017). In this study, the biomass productivity of 8.0 g m^{-2} d^{-1} was equivalent to a
310 volumetric biomass productivity of 0.18 g L d^{-1}, which exceeds previous values
311 reported for open systems.
312
313 **3.2. High-value algal biomass production from flue-gas**
314 Microalgae are capable of producing high-energy compounds, which can contribute to
315 the economic viability of the photosynthetic CO_2 removal processes either from biogas
316 or flue-gas. Carbohydrates accumulation triggered by nitrogen starvation is one of the
317 most effective ways to obtain added-value biomass (Ho *et al*., 2015). It is important to
318 highlight that this operation is performed batch-wise, since a previous biomass
319 production stage is typically required before inducing such accumulation due to the
320 different nutrient requirements of both biochemical processes. In this sense, the concept
321 of "survival of the fattest" introduced by Mooij *et al*. (2013) was here applied as a
322 strategy to induce the continuous accumulation of high-energy storage compounds in
323 the produced microalgae while cleaning flue-gas.
324 In stage IB, the biogas fed during operation stages IA-IIIA was replaced by a synthetic
325 flue-gas containing 20% of CO_2; therefore, the mineral medium was modified
326 accordingly in order to balance the carbon/nitrogen load to keep the same assimilative
327 nutrient removal reached in *section 3.1.2*. Consequently, the nutrient solution was fed at
328 an HRT of 15 days and the system was operated until constant biomass concentration of
329 1.5 ± 0.0 g L^{-1} was achieved. Under steady conditions, ~100% of the N-NO_3 fed and the
330 C-CO_2 removed from flue-gas were recovered as biomass (Table 2). The harvested
331 biomass, corresponding to the total effluent obtained at the end of the alimentation

period (*i.e.* after the light period), reached 8.3 ± 0.2 g m^{-2} d^{-1}, with a composition of ~22.1% carbohydrates, 48.3 % proteins and 14.6 % ashes (Table 3).

During stage IIB, the nitrogen source was removed from the mineral medium while maintaining the same nutrients load (Figure 3). The latter strategy was implemented in order to decrease the nitrogen concentration in the cultivation broth to a non-assimilative concentration of ~1.3 mg-N L^{-1} in which the accumulation of high-energy compounds such as lipids and/or carbohydrates can occur (Figure 3).

Once N concentrations <2 mg-N L^{-1} were achieved in the cultivation broth, the mineral medium was supplemented with N-NO_3 and fed only during the dark period at the required nitrogen load to keep the same biomass productivity of that recorded in stage IIB (Table 2). As can be observed from Figure 3, microalgae were initially not able to consume the nitrogen in the absence of light (days 297-320 of stage IIIB). This can be explained by the fact that nitrogen assimilation requires the fixed CO_2 and the energy generated in the photosynthetic process. Moreover, to assimilate nitrate, the molecule has to be transported across the membrane and be reduced to ammonia, consuming in the process large amounts of energy, carbon, and protons (Perez-Garcia *et al*., 2011). After this initial adaptation period of ~20 days, consumption of the supplied nitrogen during the dark phase was observed from day 320 onwards. This fact was attributed to the concomitant degradation of storage starch in the dark period. This phenomenon would require a regenerative cycling of adenine nucleotides and phosphate that can be supported by chlororespiration, which plays an important role in the dark recovery of plants from photoinhibition through *de novo* protein synthesis (Beardall *et al*., 2003). It has been suggested that chlororespiration supplies ATP for maintenance and synthetic processes in chloroplasts in the dark, supplementing ATP from glycolysis in the plastids (Raven and Beardall, 2003). Therefore, the accumulated high-energy molecules in the

form of glucose-based carbohydrates might be oxidized through the Embden–Meyerhof pathway and/or the Pentose Phosphate pathway, the energy production routes (NADPH, ATP), during the dark period. In that way, enzymes involved in nitrate assimilation (nitrate reductase and nitrite reductase) that work sequentially, had the required energy to catalyze nitrate to ammonium in the dark period; while during the light period CO_2 is reduced to carbohydrates through the Calvin cycle. This hypothesis was supported by the higher carbohydrate content recorded by the end of the light period, *i.e*. the 12 h nitrogen famine period, in contrast to that recorded by the end of the dark period, *i.e*. the 12 h nitrogen supplementation period (Table 3).

Similar results were observed during stage IVB, when the mineral medium was replaced by an anaerobic digestate but keeping the same nitrogen ($N\text{-}NH_4^+$) load. At this point, it is worth noticing that the variation in biomass productivity observed in stage IVB was likely due to the decrease in CO_2 removal down to 91.6± 11.3%, driven by the lower pH as a result of ammonium feeding. Furthermore, during this period the occurrence of *Pseudanabaen*a sp. (12%) was recorded which was attributed to lack of aseptic conditions of the digestate. This fact is frequently reported in open systems where rapid variations in microalgae population are expected. Moreover, the appearance of this cyanobacterium has been previously reported in wastewater treatment processes coupled to biogas upgrading (Serejo *et al*., 2015).

Finally, carbohydrates productivities ~3 g m^{-2} d^{-1} were recorded under the N-dark feeding strategies, which represents 1.7 times the productivity reached under normal nutrition conditions (Figure 4). The high concentration of carbohydrates reached is preferred for its chemical or biological valorization, for instance as the substrate for biohydrogen by dark-fermentation (Chen *et al*., 2016), ethanol (John *et al*., 2011) or biogas production (Zamalloa *et al*., 2011). Furthermore, the biomass production through

382 wastewater treatment significantly contributes to the flue-gas or biogas cleaning process
383 (Toledo-Cervantes *et al*., 2017a.). These results confirm the feasibility of applying this
384 novel strategy for inducing the accumulation of high-energy storage compounds during
385 the photosynthetic abatement of CO_2 coupled with wastewater treatment, since it allows
386 for a continuous production of added-value algal biomass.
387
388 **4. Conclusions**
389 To the best of our knowledge, this is the first experimental study reporting the long-term
390 performance of a tubular photobioreactor for the abatement of CO_2 from exhaust gases
391 (biogas and flue-gas) coupled with algal biomass production. The system here proposed
392 showed an efficient removal of CO_2 from gas streams (>98%), the upgraded biogas
393 composition meeting the required standards for electricity production. Moreover, the
394 innovative nutrient supplementation strategy, *i.e.* feeding nutrients during the dark
395 period, allowed enhancing the carbohydrates content in the produced biomass by 1.7
396 times regardless of the nitrogen source. In summary, this study confirmed the potential
397 of the photosynthetic CO_2 removal process in closed photobioreactors to support
398 nutrient recovery from digestate and production of added-value biomass with high
399 carbohydrates content, resulting in a cost-efficient and environmentally-friendly
400 technology.
401
402 **Acknowledgments**
403 This work was supported by the research grants of the Fundación Iberdrola, the
404 Regional Government of Castilla y León (UIC 71), MINECO and the European Union
405 through the FEDER program (CTM2015-70722-R). CONACyT-México is gratefully
406 acknowledged for the Postdoctoral grant of Alma Toledo (No. Reg: 237873).

References

1. Arbid Z., Ruiz J., Álvarez-Díaz P., Garrido-Pérez C., Barragán J., Perales J. A., Effect of pH control by means of flue gas addition on three different photo-bioreactors treating urban wastewater in long-term operation. *Ecol. Eng.* **2013**, 57: 226-235.

2. Beardall, J., Quigg, A., & Raven, J. A. 2003. Oxygen consumption: photorespiration and chlororespiration. In Photosynthesis in algae. pp. 157-181. Springer Netherlands.

3. Chisti, Y., Biodiesel from microalgae. *Biotechnol. Adv*. **2007**, 25: 294–306.

4. Chen, C. Y., Chang, H. Y., & Chang, J. S. Producing carbohydrate-rich microalgal biomass grown under mixotrophic conditions as feedstock for biohydrogen production. International journal of hydrogen energy, **2016**, 41(7), 4413-4420.

5. Perez-Garcia, O., Escalante, F. M., de-Bashan, L. E., Bashan, Y. Heterotrophic cultures of microalgae: metabolism and potential products. Water research, **2011**, 45(1), 11-36.

6. Dubois, M., Gilles, K.A., Hamilton, J.K., Rebers, P.A., Smith, F., Colorimetric method for determination of sugars and related substances. Anal. Chem. **1956**, 28:, 350–356.

7. Eaton, A.D., Clesceri, L.S., Greenberg, A.E. Standard Methods for the Examination of Water and Wastewater, 21st ed. American Public Health Association/American Water Works Association/Water Environment Federation, Washington, DC, 2005.

8. Franco-Morgado, M., Alcántara, C., Noyola, A., Muñoz, R., González-Sánchez, A., A study of photosynthetic biogas upgrading based on a high rate algal pond under

alkaline conditions: Influence of the illumination regime. *Sci. Total Environ*. **2017**, 592: 419–425.

9. González-Sánchez, A., and Posten C. Fate of H_2S during the cultivation of *Chlorella* sp. deployed for biogas upgrading. *J. Environ. Manage.* **2017**, 191: 252-257.

10. Grobbelaar, J.U. 2013. Inorganic Algal Nutrition, in: Richmond, A., and Hu, Q. (Eds), Handbook of Microalgal Culture: Applied Phycology and Biotechnology; 2nd edition, John Wiley & Sons, UK, pp 123-133

11. Ho, S. H., Huang, S. W., Chen, C. Y., Hasunuma, T., Kondo, A., & Chang, J. S. Characterization and optimization of carbohydrate production from an indigenous microalga Chlorella vulgaris FSP-E. Bioresource Technology, **2013**, 135, 157-165.

12. John, R. P., Anisha, G. S., Nampoothiri, K. M., & Pandey, A. Micro and macroalgal biomass: a renewable source for bioethanol. *Bioresource technology*, **2011**, 102(1), 186-193.

13. López J.C., Quijano G., Souza T.S.O., Estrada J.M., Lebrero R., Muñoz R. Biotechnologies for greenhouse gases (CH_4, N_2O, and CO_2) abatement: state of the art and challenges. *Appl Microbiol Biotechnol*, **2013**, 97: 2277–2303.

14. Lowry, O., Rosenbrough, N., Farr, A., Randall, R., Protein measurement with the folin phenol reagent. *J. Biol. Chem*. **1951**, 193: 265−275.

15. Meier, L., Barros, P., Torres, A., Vilchez, C., Jeison, D. Photosynthetic biogas upgrading using microalgae: Effect of light/dark photoperiod. Renewable Energy, **2017**, 106, 17-23.

16. Mooij, P.R., Stouten, G.R.; Tamis, J.; van Loosdrecht, M.C.M., Kleerebezem R., Survival of the fattest. Energy Environ. Sci., **2013**, 6(12): 3404-3406.

17. Mooij, P.R., de Graaff, D.R., van Loosdrecht, M.C.M., Kleerebezem R., Starch productivity in cyclically operated photobioreactors with marine microalgae—effect of ammonium addition regime and volume exchange ratio. *J Appl Phycol*, **2015**, 27: 1121.

18. Muñoz R., Meier L., Díaz I., Jeison D., A review on the state-of-the-art of physical/chemical and biological technologies for biogas upgrading, *Rev. Environ. Sci. Biotechnol*. **2015**, 14(4): 727-759.

19. Park J.B.K., Craggs R.J., Wastewater treatment and algal production in high rate algal ponds with carbon dioxide addition, *Wat. Sci. Technol*. **2010**, 61: 633–639.

20. Posadas, E., Marín, D., Blanco, S., Lebrero, R., & Muñoz, R. Simultaneous biogas upgrading and centrate treatment in an outdoors pilot scale high rate algal pond. Bioresource Technology, **2017**, 232, 133-141.

21. Posadas E., Morales M. M., Gómez C., Acién F. G., Muñoz R., Influence of pH and CO_2 source on the performance of microalgae-based secondary domestic wastewater treatment in outdoors pilot raceways, *Chem. Eng. J.* **2015**, 265: 239-248.

22. Raeesossadati M.J., Ahmadzadeh H., McHEnry M.P., Moheimani N.R. CO_2 bioremediation by microalgae in photobioreactors: Impacts of biomass and CO_2 concentrations, light, and temperature, *Algal Res*. **2014**, 6: 78-85.

23. Raven, J. A., Beardall, J. 2003. Carbohydrate metabolism and respiration in algae. In Photosynthesis in algae. pp. 205-224. Springer Netherlands.

24. Sander R. Compilation of Henry's Law Constants for Inorganic and Organic Species of Potential importance in Environmental Chemistry 1999.

25. Serejo, M.L., Posadas, E., Boncz, M.A., Blanco, S., García-Encina, P., Muñoz, R., Influence of biogas flow rate on biomass composition during the optimization of biogas upgrading in microalgal-bacterial processes. *Environ. Sci. Technol*. **2015**, 49: 3228–3236.

26. Toledo-Cervantes A., Serejo M., Blanco S., Pérez R., Lebrero R., Muñoz R., Photosynthetic biogas upgrading to bio-methane: boosting nutrient recovery via biomass productivity control. *Algal Res*., **2016**, 17: 56-52.

27. Toledo-Cervantes, A., Estrada, J. M., Lebrero, R., Muñoz, R. A comparative analysis of biogas upgrading technologies: Photosynthetic vs physical/chemical processes. *Algal Res*., **2017a**. 25: 237-243.

28. Toledo-Cervantes, A., Madrid-Chirinos, C., Cantera, S., Lebrero, R., Muñoz, R. Influence of the gas-liquid flow configuration in the absorption column on photosynthetic biogas upgrading in algal-bacterial photobioreactors, *Bioresour. Technol*, **2017b**, 225: 336-342.

29. United Nations (2015) Climate change (Last access: March 2017): http://www.cop21.gouv.fr/en/

30. Warmuzinski K., Tanczyk M., Jaschik M., Experimental study on the capture of CO_2 from flue gas using adsorption combined with membrane separation, *Int. J. Greenh. Gas Con*. **2015**, 37: 182-190.

31. World Bank. 2014. World Development Indicators: Energy dependency, efficiency and carbon dioxide emission, (Last access: March 2017): http://wdi.worldbank.org/table/3.8

32. Zamalloa, C., Vulsteke, E., Albrecht, J., & Verstraete, W. The techno-economic potential of renewable energy through the anaerobic digestion of microalgae. *Bioresource technology*, **2011**, *102*(2), 1149-1158.

500 **Figure captions**

501

502 **Figure 1.** Schematic diagram of the experimental system used for the photosynthetic
503 CO_2 removal from biogas and flue-gas.

504 **Figure 2.** Time course of **a)** the CO_2 (○) and H_2S (▲) removal efficiencies; and **b)** the
505 upgraded biogas composition CH_4 (●), CO_2 (■), N_2 (□) and O_2 (+).

506 **Figure 3.** Time course of the total nitrogen (TN) concentration in the cultivation broth.
507 Open circles represent the nitrogen concentration at the end of the dark period where the
508 nitrogen supplementation took place (8:00 am) and solid squares represent the nitrogen
509 concentration at the end of the illuminated period (8:00 pm).

510 **Figure 4.** Biomass concentration (■) and carbohydrates productivity (white bars)
511 achieved under different N-supplementation strategies.

Table 1. Abiotic removal efficiencies and upgraded biogas composition obtained at different liquid to biogas flow rate ratios (L/G).

	Removal efficiencies (%)		Upgraded biogas composition (%)				
L/G	**H_2S**	**CO_2**	**CH_4**	**H_2S**	**CO_2**	**N_2**	**O_2**
1	88.2 ± 1.3	61.6 ± 3.1	84.1 ± 0.4	0.05 ± 0.0	10.6 ± 1.1	4.1 ± 1.0	2.2 ± 0.1
4	93.2 ± 0.4	76.6 ± 1.5	85.9 ± 0.6	0.03 ± 0.0	6.7 ± 0.1	6.0 ± 0.7	3.5 ± 0.2
7	95.5 ± 1.3	89.6 ± 2.3	81.3 ± 0.3	0.02 ± 0.0	3.1 ± 0.4	14.3 ± 2.5	6.5 ± 0.9
11	98.6 ± 0.9	90.8 ± 3.0	82.8 ± 0.1	0.01 ± 0.0	2.7 ± 1.2	13.2 ± 2.5	7.1 ± 0.5

Table 2. Average values for operating parameters recorded during flue-gas cleaning.

Stage	pH	DO ($mg\text{-}O_2\ L^{-1}$)	Productivity ($g\ m^{-2}\ d^{-1}$)	CO_2 removal (%)
IB	10.1 ± 0.1	10.7 ± 0.8	8.3 ± 0.2	99.8 ± 0.7
IIB	10.5 ± 0.4	8.7 ± 0.3	6.7 ± 0.1	99.3 ± 0.1
IIIB	10.4 ± 0.2	6.0 ± 0.2	6.8 ± 0.3	99.3 ± 0.0
IVB	9.3 ± 0.4	6.2 ± 0.3	5.8 ± 0.4	91.1 ± 1.4

Table 3. Biochemical composition of algal biomass under different nutrition strategies

Stage	I-IIB (Regular nutrition)	IIIB		IVB	
		N-famine - light	$N\text{-}NO_3^-$ - dark	N-Famine - light	$N\text{-}NH_4^+$ - dark
Carbohydrates (mg g_b^{-1})	221.4 ± 56.2	439.9 ± 32.3	369.7 ± 27.9	453.6 ± 58.1	378.3 ± 11.9
Proteins (mg g_b^{-1})	482.9 ± 57.7	349.4 ± 53.0	526.0 ± 18.0	424.4 ± 54.7	476.8 ± 26.6
Lipids (mg g_b^{-1})	48.5 ± 3.9	40.0 ± 4.2	48.0 ± 2.5	31.5 ± 5.7	31.6 ± 3.8
Ashes (mg g_b^{-1})	146.0 ± 1.2	70.0 ± 0.0	40.0 ± 0.3	76.0 ± 0.1	56.8 ± 0.0

Figure 1

Click here to download high resolution image

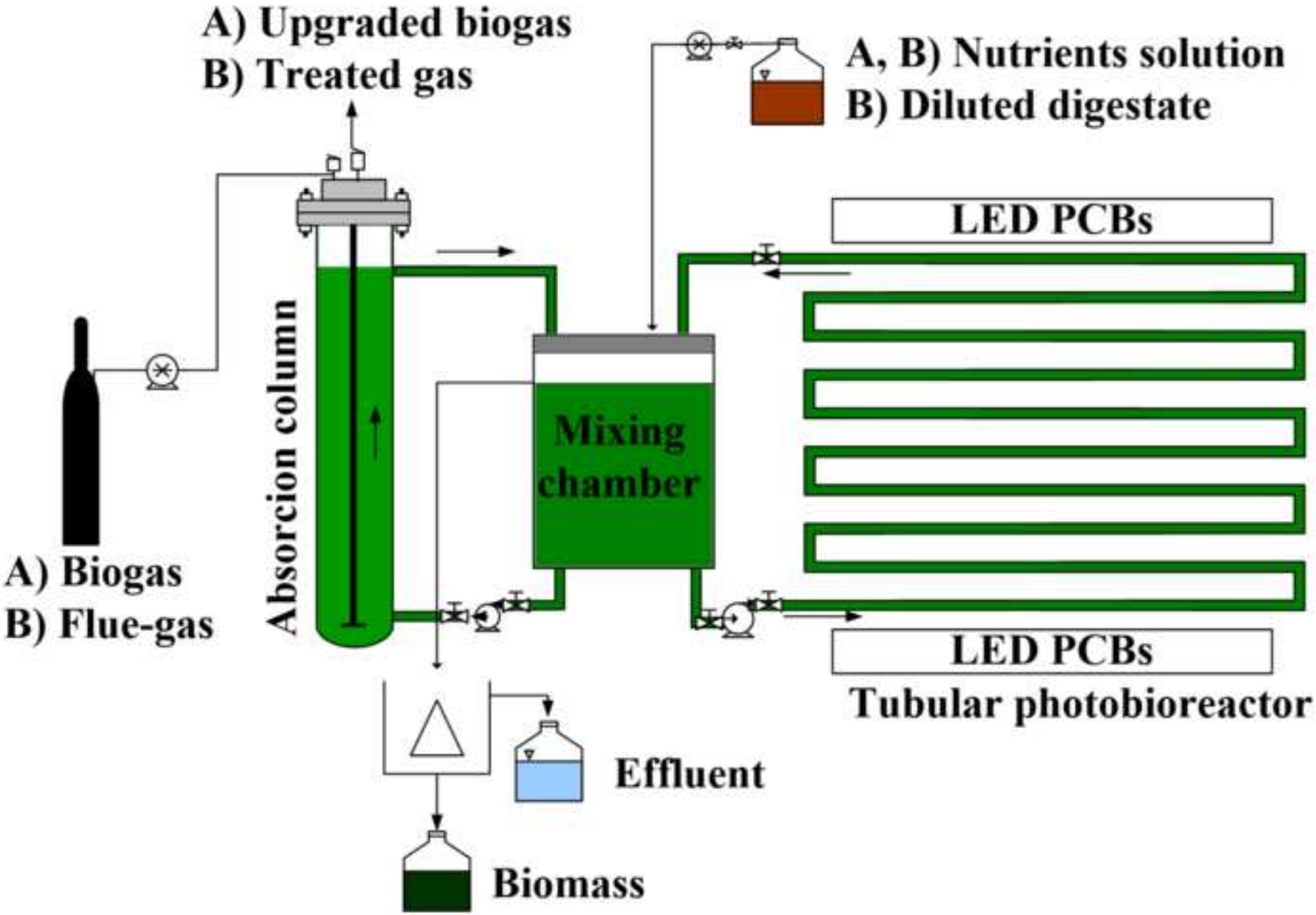

Figure 2

Click here to download high resolution image

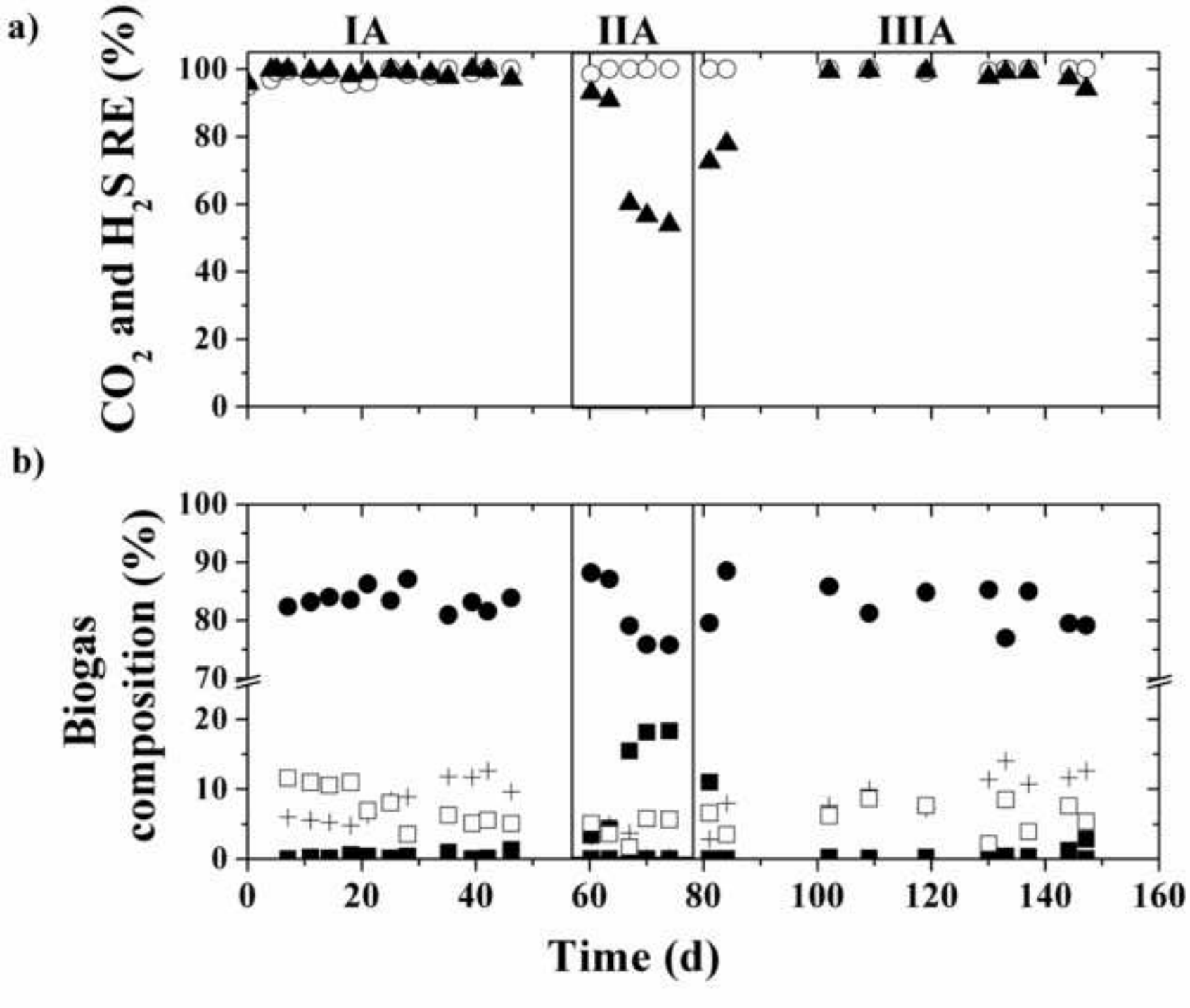

Figure 3

Click here to download high resolution image

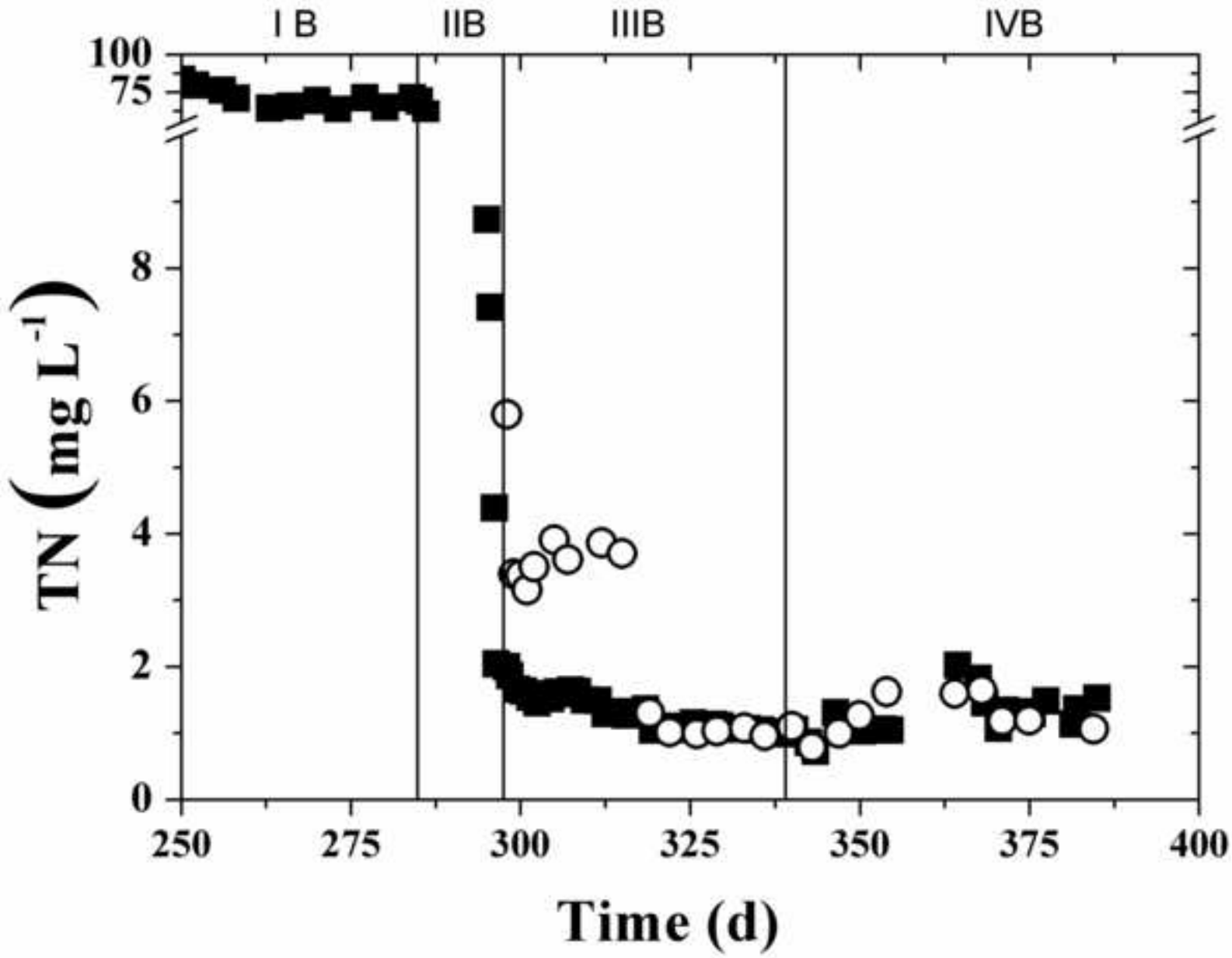

Figure 4

Click here to download high resolution image

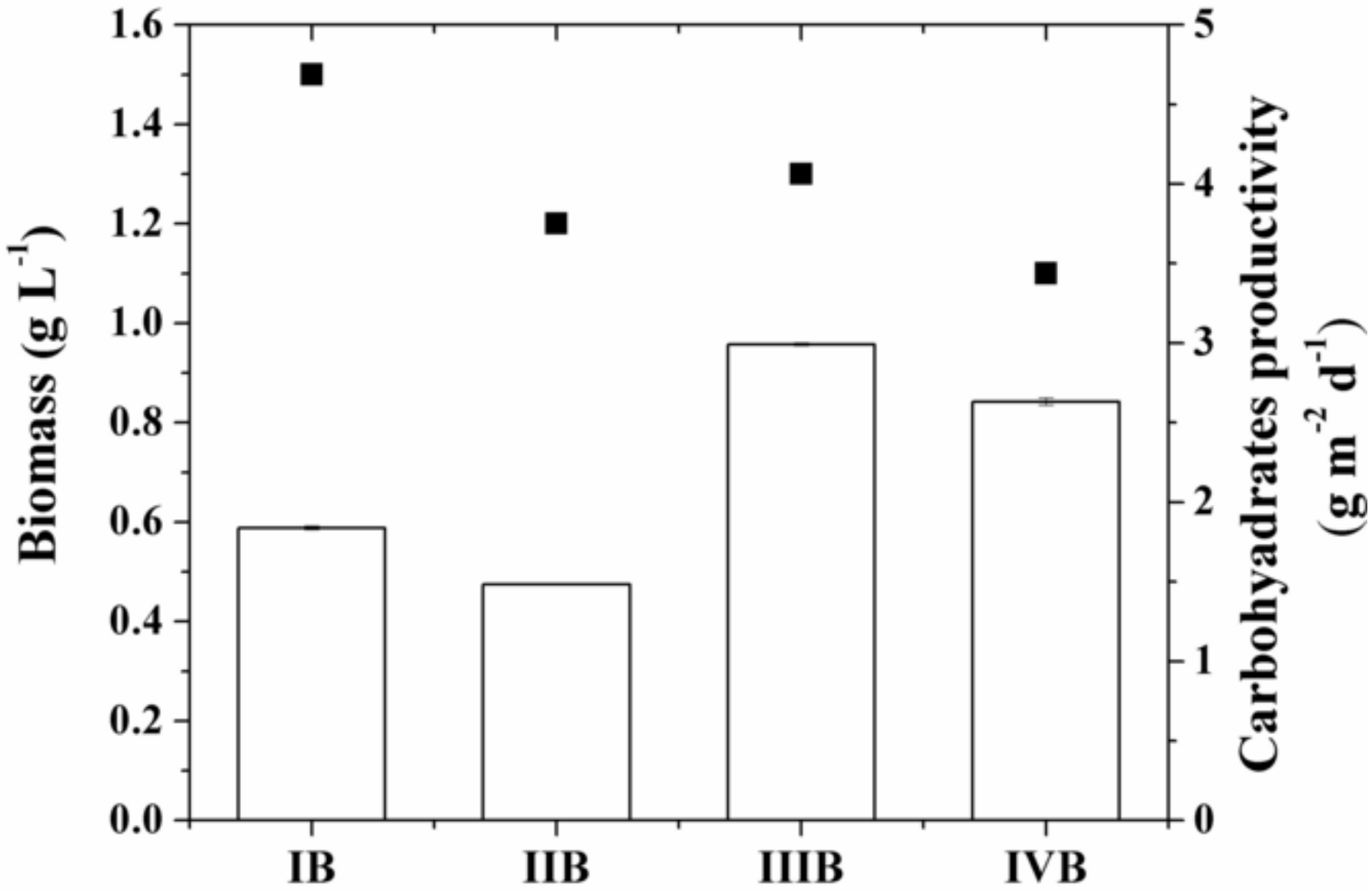

Data Statement

Click here to download Data Statement: dataprofile.xml